



Transcriptome-based repurposing of apigenin as a potential anti-fibrotic agent targeting hepatic stellate cells

Citation

Hicks, D. F., N. Goossens, A. Blas-García, T. Tsuchida, B. Wooden, M. C. Wallace, N. Nieto, et al. 2017. "Transcriptome-based repurposing of apigenin as a potential anti-fibrotic agent targeting hepatic stellate cells." *Scientific Reports* 7 (1): 42563. doi:10.1038/srep42563. <http://dx.doi.org/10.1038/srep42563>.

Published Version

doi:10.1038/srep42563

Permanent link

<http://nrs.harvard.edu/urn-3:HUL.InstRepos:32071894>

Terms of Use

This article was downloaded from Harvard University's DASH repository, and is made available under the terms and conditions applicable to Other Posted Material, as set forth at <http://nrs.harvard.edu/urn-3:HUL.InstRepos:dash.current.terms-of-use#LAA>

Share Your Story

The Harvard community has made this article openly available.
Please share how this access benefits you. [Submit a story](#).

[Accessibility](#)

SCIENTIFIC REPORTS



OPEN

Transcriptome-based repurposing of apigenin as a potential anti-fibrotic agent targeting hepatic stellate cells

Received: 30 November 2016

Accepted: 10 January 2017

Published: 03 March 2017

Daniel F. Hicks¹, Nicolas Goossens^{1,2}, Ana Blas-García^{1,3}, Takuma Tsuchida^{1,4}, Benjamin Wooden¹, Michael C. Wallace^{1,5}, Natalia Nieto⁶, Abigale Lade¹, Benjamin Redhead⁷, Arthur I Cederbaum⁸, Joel T. Dudley⁷, Bryan C. Fuchs⁹, Youngmin A. Lee¹, Yujin Hoshida¹ & Scott L. Friedman¹

We have used a computational approach to identify anti-fibrotic therapies by querying a transcriptome. A transcriptome signature of activated hepatic stellate cells (HSCs), the primary collagen-secreting cell in liver, and queried against a transcriptomic database that quantifies changes in gene expression in response to 1,309 FDA-approved drugs and bioactives (CMap). The flavonoid apigenin was among 9 top-ranked compounds predicted to have anti-fibrotic activity; indeed, apigenin dose-dependently reduced collagen I in the human HSC line, TWNT-4. To identify proteins mediating apigenin's effect, we next overlapped a 122-gene signature unique to HSCs with a list of 160 genes encoding proteins that are known to interact with apigenin, which identified *C1QTNF2*, encoding for Complement C1q tumor necrosis factor-related protein 2, a secreted adipocytokine with metabolic effects in liver. To validate its disease relevance, *C1QTNF2* expression is reduced during hepatic stellate cell activation in culture and in a mouse model of alcoholic liver injury *in vivo*, and its expression correlates with better clinical outcomes in patients with hepatitis C cirrhosis ($n = 216$), suggesting it may have a protective role in cirrhosis progression. These findings reinforce the value of computational approaches to drug discovery for hepatic fibrosis, and identify *C1QTNF2* as a potential mediator of apigenin's anti-fibrotic activity.

The hepatic stellate cell (HSC) represents the major focus for developing anti-fibrotic therapies, whereas other cell types, e.g. portal fibroblasts, also contribute to fibrogenesis to a minor extent depending on the site, duration and nature of liver injury^{1,2}. HSC-specific genes and proteins likely serve as clues to candidate therapeutic targets and will accelerate preclinical testing and clinical development of anti-fibrotic therapies.

Bioinformatic interrogation of public databases is a comprehensive and efficient strategy to identify disease molecular signatures, drug targets, and even candidate drugs. There are a growing number of transcriptome datasets available for the identification of genes and pathways unique to a variety of biological and clinical contexts across multiple assay formats and tissue types, including liver³. Liver disease-specific molecular signatures such as regulators of collagen deposition and hepatocellular carcinoma subtype/prognosis classifiers have been identified to date⁴⁻⁷. Our previous unbiased interrogation of the liver cell transcriptome compendium has identified a 122-gene HSC-specific molecular signature uniquely expressed in quiescent and/or activated HSCs compared to

¹Division of Liver Diseases, Department of Medicine, Liver Cancer Program, Tisch Cancer Institute, Graduate School of Biomedical Sciences, Icahn School of Medicine at Mount Sinai, New York, USA. ²Division of Gastroenterology and Hepatology, Geneva University Hospital, Geneva, Switzerland. ³Department of Pharmacology, University of Valencia-FISABIO, Valencia, Spain. ⁴Research Division, Mitsubishi Tanabe Pharma Corporation, Saitama, Japan. ⁵University of Western Australia, West Leederville, WA, Australia. ⁶Department of Pathology, University of Illinois at Chicago, Chicago, USA. ⁷Department of Genetics and Genomics Sciences, Icahn School of Medicine at Mount Sinai, New York, USA. ⁸Department of Pharmacology and Systems Therapeutics, Icahn School of Medicine at Mount Sinai, New York, USA. ⁹Division of Surgical Oncology, Massachusetts General Hospital Cancer Center, Harvard Medical School, Boston, USA. Correspondence and requests for materials should be addressed to Y.H. (email: yujin.hoshida@mssm.edu) or S.L.F. (email: scott.friedman@mssm.edu)

other cell types in the liver, which was associated with poorer clinical outcome in patients with hepatitis C virus (HCV)-related cirrhosis and hepatocellular carcinoma⁸.

In parallel, molecular signature-based *in silico* drug screening and repurposing has been successfully utilized for quick hypothesis-free identification of novel therapeutics for a variety of cancers and inflammatory diseases, among many others diseases³. In the current study, we used an experimentally-defined HSC activation gene signature in an unbiased manner as a basis for applying a computational drug discovery approach to identify candidate anti-fibrotic drugs that antagonize the HSC gene signature.

Material and Methods

Computational compound screen for candidate anti-fibrotic agents. An HSC activation signature was defined in transcriptome profiles of freshly isolated HSCs from cirrhotic rat liver treated with repeated low-dose diethylnitrosamine (low-dose DEN rat)⁹ (NCBI Gene Expression Omnibus [GEO] accession number, GSE63726). Differentially expressed genes between the cells isolated from cirrhotic and healthy control livers were defined after making to human orthologous genes (NCBI HomoloGene database, release 68) by random permutation t-test based on significance threshold of false discovery rate (FDR < 0.05) (Supplementary Table 1). The gene signature was used to query a database of transcriptome profiles of 1,309 unique FDA-approved drugs and bioactive compounds, the Connectivity Map (CMap) database (<https://portals.broadinstitute.org/cmap/>)¹⁰. Compounds with significant negative association (enrichment $p \leq 0.05$) were selected as candidates for subsequent experimental evaluation.

***In vitro* assessment of candidate anti-fibrotic agents.** TWNT-4 (human HSC line) cells¹¹ were seeded onto a 96-well plate at 5,000 cells per well in 100 μ l of assay medium (DMEM, 10% FBS, 1% penicillin/streptomycin), and cultured at 37 °C and 5% CO₂. After 24 hours, the cells were treated with apigenin (Sigma-Aldrich) ($\geq 97\%$ purity) at final concentrations of 2.5 μ M, 10 μ M, 20 μ M, 40 μ M, 60 μ M, 80 μ M, 100 μ M, and 200 μ M dissolved in 0.5% DMSO or DMSO control in triplicate for 24 hours. Cell viability was measured by MTS assay using CellTiter 96[®] Aqueous One Solution Reagent (Promega) following manufacturer's instruction. Percentage of mean absorbance of each drug-treated condition over the control was calculated.

Quantitative reverse transcriptase polymerase chain reaction (qRT-PCR). RNA was extracted from adherent cells using RNeasy Mini kit (Qiagen). Equimolar concentrations of RNA were converted to cDNA (Clontech), and quantitative real-time PCR was performed using SYBR green reagent (Roche) on the Lightcycler 480 system (Roche). Gene expression level in each sample was internally normalized to *GAPDH* expression. The following PCR primers were used (5' to 3'): GGCTTCCCTGGTCTTCCTGG (forward) and CCAGGGGTCCAGCCAAT (reverse) for human *COL1A1*; GAGGCTCCTCCCAGTCATCA (forward) and GGGATCATGGTGGTTACCCAGA (reverse) for human *C1QTNF2*; CCAGAAGCCATCAGCAGCAAG (forward) and AGGCCCTGAGAGATCTGTGG (reverse) for human *PDGFRB*; AGGCACCCCTGAACCCCAA (forward) and CAGCACCGCCTGGATAGCC (reverse) for human *ASMA*; CAAGGGCTACCATGCCAACT (forward) and AGGGCCAGGACCTTGCTG (reverse) for human *TGFBI*; CGAGTGCCAAATGAAGAGGACC (forward) and AAACCTGAGCCAGAACCTGACG (reverse) for human *TGFRB1*; CAATGACCCCTTCATTGACC (forward) and GATCTCGCTCCTGGAAGATG (reverse) for human *GAPDH*.

Western blotting. TWNT-4 cells were lysed in RIPA buffer (150 mM NaCl, 50 mM Tris-HCl, 1% IGEPAL, 0.5% Sodium deoxycholate, 1% SDS) with proteinase inhibitors (Roche) and pelleted. Inguinal adipose tissue was dissected from two C57BL/6 mice (Charles River). Whole liver tissue was isolated from 5 control mice fed a normal diet for 6 weeks and 5 mice fed a Lieber DeCarli ethanol-containing diet for 6 weeks. In both cases, the tissue was lysed mechanically using steel beads in a TissueLyser LT (Qiagen) and with RIPA lysis buffer with the proteinase inhibitor. The lysate was sonicated and pelleted and the aqueous supernatant was isolated. Twenty μ g of protein from each sample was suspended in NuPAGE LDS sample buffer and heated for 10 min at 70 °C. Samples were electrophoresed on 10% BisTris NuPAGE gels (Invitrogen) and then transferred to nitrocellulose membranes (Invitrogen). Membrane blotting was performed using the following primary antibodies, rabbit polyclonal anti-COL1A1 antibody (Rockland, Limerick, PA, catalog #600-401-103) (1:5000), rabbit polyclonal anti-C1QTNF2 antibody (ProSci, catalog #3561) (1:1000), mouse monoclonal anti-GAPDH antibody (Millipore, catalog #CB1001) (1:2500), mouse monoclonal anti- β -tubulin (Sigma-Aldrich, catalog #T4026) (1:2500), mouse anti-calnexin (Abcam, catalog #75801) (1:2500) and appropriate HRP-conjugated secondary antibody. Bands were visualized with chemiluminescent HRP antibody detection reagent (HyGlo e2400, Denville), captured with Amersham Imager 600 (GE Healthcare Life Sciences), and quantified using ImageJ software (<https://imagej.nih.gov/ij/>).

Immunofluorescence staining. A total of 50,000 TWNT-4 cells were plated onto glass coverslips and cultured until 90% confluent, and then fixed with 100% acetone for 10 minutes at -20 °C. The cells were subsequently permeabilized in Tween-20 detergent in PBS for 20 minutes and then incubated in the rabbit polyclonal anti-C1QTNF2 antibody (1:1000) with negative and positive controls, chicken polyclonal anti-GFAP (Abcam, catalog #4674) (1:200), and anti-Desmin (AbCam, catalog #15200) (1:200). Appropriate green fluorescent tagged secondary antibodies (Life Technologies) were used and DAPI was used for nuclear staining. Cells were imaged under Eclipse TS100 fluorescent microscope (Nikon).

Culture activated mouse HSCs. DNA microarray-based transcriptome profiles of mouse primary HSCs before (day 0) and after *in vitro* culture activation (day 7) were obtained from GEO database (NCBI Gene Expression Omnibus [GEO] accession number, GSE34949)^{12,13}.

Drug	Enrichment score	p value	Regulatory approval	Test in human	Known adverse effects	Published anti-fibrotic effect
leflunomide	-0.20	0.002	Yes	Yes ²⁹	Diarrhea, nausea, alopecia, rash ²⁹	No
AH-23848	-0.19	0.005	No	Yes ³⁰	Heartburn, nausea, vomiting ³¹	No
xamoterol	-0.18	0.008	No	Yes ³²	Nausea ³²	No
6-benzylaminopurine	-0.18	0.01	No	No	Uncertain	No
irinotecan	-0.17	0.015	Yes	Yes ³³	Bone marrow suppression, diarrhea, alopecia, fatigue, nausea, vomiting ³³	No
hydroxyachillin	-0.17	0.015	No	No	Uncertain	No
aceclofenac	-0.17	0.024	Yes	Yes ³⁴	Moderate epigastric discomfort and dyspepsia ³⁴	Yes ³⁵
methylergometrine	-0.16	0.028	Yes	Yes ³⁶	Rare Acute Coronary Syndrome, Myocardial Infarction ³⁷	No
CP-863187 ³⁸	-0.16	0.036	No	No	Uncertain	No
estrone	-0.16	0.028	Yes	Yes ³⁹	CHD, stroke, breast cancer, PE ³⁹	No
apigenin	-0.16	0.041	No	Yes ⁴⁰	Uncertain	Yes ^{16,17}
PHA-00767505E ⁴¹	-0.16	0.053	No	No	Uncertain	No
digoxigenin	-0.16	0.045	No	No	Uncertain	No
5252917 ⁴²	-0.16	0.031	No	No	Uncertain	No
3-aminobenzamide	-0.16	0.04	No	No	Uncertain	Yes ⁴³
zuclopenthixol	-0.16	0.042	Yes	Yes ⁴⁴	Extra-pyramidal symptoms ⁴⁴	No
bucladesine	-0.16	0.054	No	Yes ^{45,46}	Vasodilation ^{45,46}	Yes ⁴⁷
erastin	-0.15	0.048	No	No	Uncertain	No

Table 1. Compounds predicted to be antifibrotic by an *in silico* screen with key pharmacological and clinical characteristics. * Approval by any international agency.

Clinical HCV cirrhosis cohort. DNA microarray-based transcriptome profiles of 216 patients with HCV-related compensated cirrhosis we previously reported were used to evaluate prognostic association of *CIQTNF2* expression level (GSE15654)⁶. *CIQTNF2*-high group was defined as samples with *CIQTNF2* expression higher than one standard deviation above mean. Prognostic association was assessed by Kaplan-Meier curve and log-rank test.

Statistical analysis. Continuous values are presented by mean and standard error of mean (SEM). Differences were assessed by either t-test or one-way ANOVA followed by Dunnett's multiple comparisons test. Two-tailed p-value less than 0.05 was regarded as statistically significant. All statistical analyses were performed using Graph Pad Prism version 7.0a (GraphPad Software).

Results

Computational screen to identify candidate anti-fibrotic agents. A 673-gene *in vivo* HSC activation signature was defined in the isolated HSC fraction from the low-dose DEN rat (Supplementary Table 1). The gene signature was used to query the compound perturbation transcriptome database (CMap) for candidate anti-fibrotic agents that potentially antagonize the HSC activation signature. Eighteen compounds with significant negative association ($p \leq 0.05$) were identified (Table 1). Of note, the majority of the compounds ($n = 14$, 78%) are not recognized for their possible anti-fibrotic effect, highlighting the potential advantage of this unbiased *in silico* screen to efficiently identify candidate drugs. Among them, 9 top hit compounds commercially available and without clinically known severe toxicity were chosen for subsequent experimental evaluation.

***In vitro* validation of anti-fibrotic effect of apigenin in a HSC cell line.** The 9 computationally prioritized candidate compounds were tested for their anti-fibrotic effect in a human HSC cell line, TWNT-4, together with a multi-kinase inhibitor, sorafenib, and an mTOR inhibitor, rapamycin, as positive controls^{14,15}. Apigenin, a flavonoid with a known anti-fibrotic activity in a mouse model of chronic pancreatitis^{16,17}, was the only compound that reduced *COL1A1* expression at comparable level to sorafenib, a known anti-fibrotic drug, with statistical significance (Fig. 1A). The *COL1A1* suppressive effect was dose-dependent (Fig. 1B), which was also confirmed at the protein level (Fig. 1C). Expression of *PDGFRB*, encoding platelet-derived growth factor receptor- β , was similarly reduced by 10 μ M of apigenin (Fig. 1D). Cell viability assessment showed that the compound is not toxic at concentrations below 20 μ M (Fig. 1E). Other known liver fibrosis-related genes, *ASMA*, *TGFB1*, and *TGFB1*, were not suppressed at the non-toxic concentration (Fig. 1F–H), suggesting that apigenin's effect is directed to a specific subset of fibrogenesis-related pathways.

***CIQTNF2* as a potential intracellular target of apigenin.** Next we sought to identify targets of apigenin in hepatic stellate cells. A 122-gene signature uniquely expressed in HSC⁸ was overlaid on a list of 160 genes encoding intracellular proteins that physically interact with apigenin based on phase display¹⁸. *CIQTNF2* was identified as the only gene common to the 2 gene lists (Fig. 2A). With 20,354 protein-coding genes in human genome according to NCBI CCDS database (release 21) (www.ncbi.nlm.nih.gov/projects/CCDS), the number of apigenin target genes (160 genes) that could be found within the hepatic stellate cell signature (122 genes) by

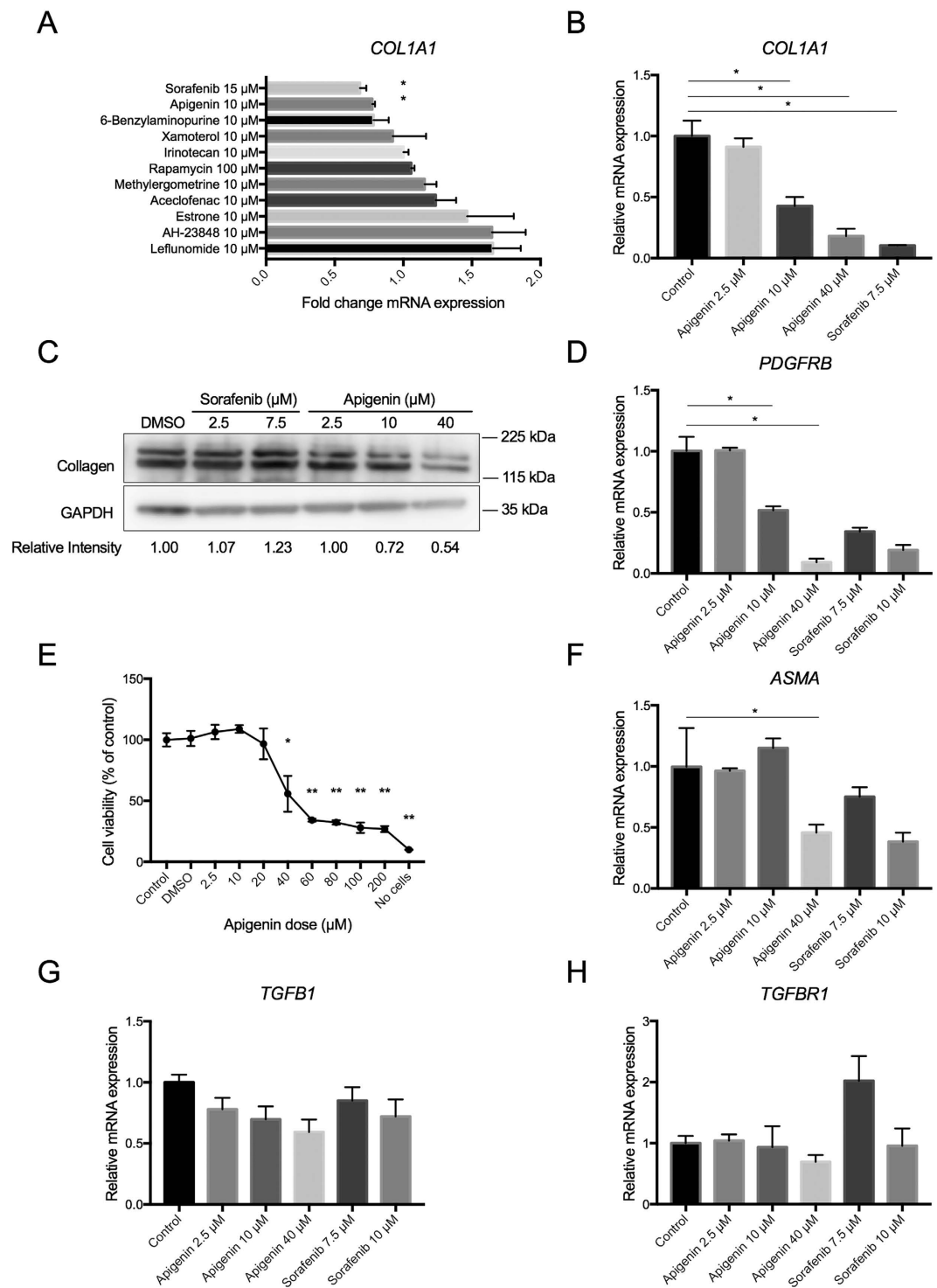


Figure 1. Anti-fibrotic effect of apigenin in human HSC line (TWNT-4 cells). (A) Modulation of *COL1A1* expression by nine computationally selected candidate compounds together with sorafenib and rapamycin (positive controls) compared to DMSO-treated controls (qRT-PCR, $n = 3$). * $p < 0.05$, t-test. (B) Dose-dependent suppression of *COL1A1* expression by apigenin (qRT-PCR, $n = 3$). * $p < 0.001$, Dunnett's test. (C) Suppression of collagen 1 protein by sorafenib and apigenin (Western blotting, $n = 1$). Relative intensity to GAPDH was calculated. (D) Modulation of *PDGFRB* expression by apigenin and sorafenib (qRT-PCR, $n = 3$). * $p < 0.001$, Dunnett's test. (E) Cell viability in association of apigenin dose (MTS assay, $n = 3$). * $p < 0.01$, ** $p < 0.001$, Dunnett's test. (F) Modulation of *ASMA* expression by apigenin and sorafenib (qRT-PCR, $n = 3$). (G) Modulation of *TGFBI* expression by apigenin and sorafenib (qRT-PCR, $n = 3$). (H) Modulation of *TGFBR1* expression by apigenin and sorafenib (qRT-PCR, $n = 3$). Bar graphs show mean and standard error of mean (SEM) (error bars) of replicated experiments.

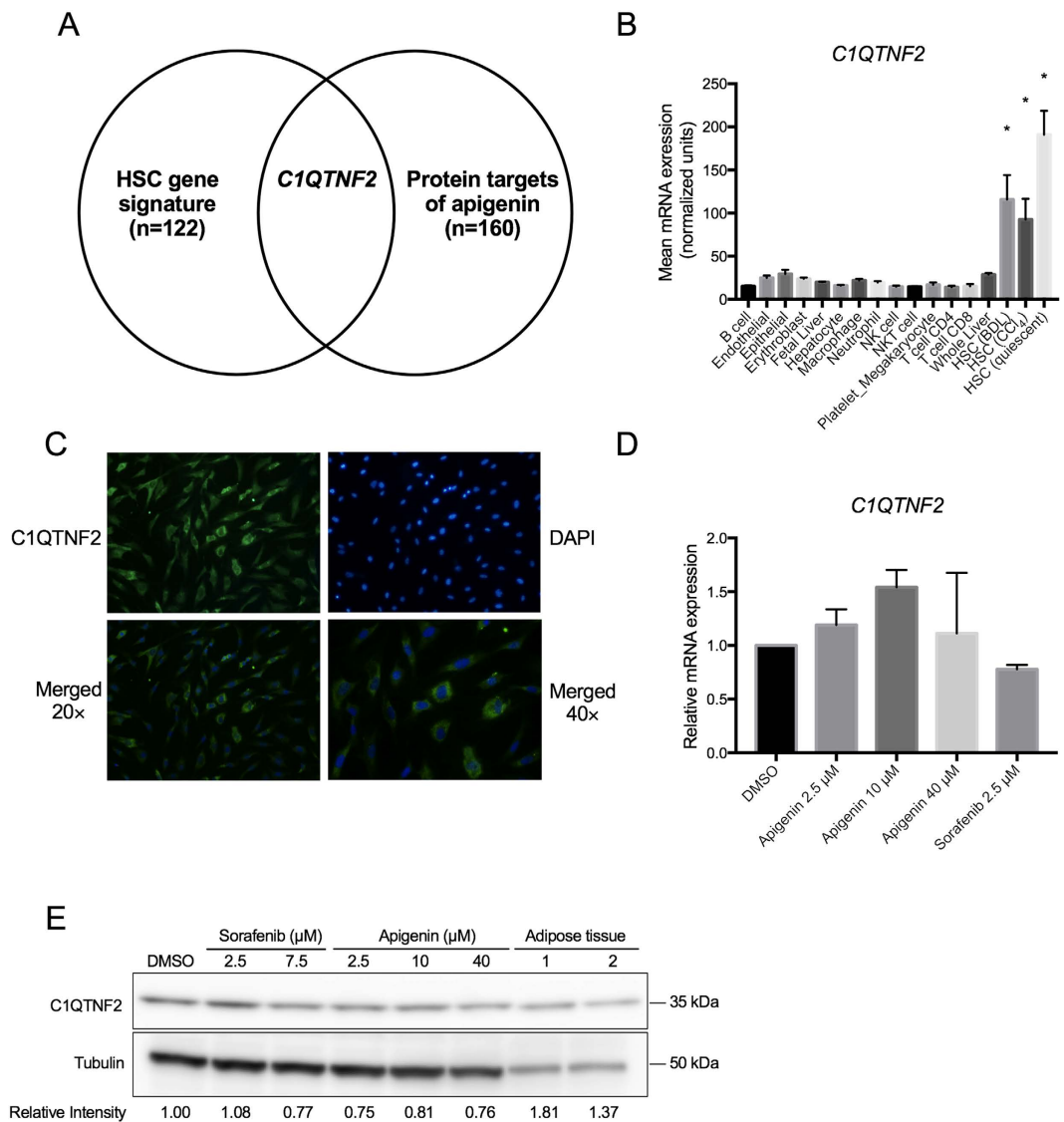


Figure 2. HSC-specific expression of *C1QTNF2*, a potential target of apigenin. (A) Overlap between HSC gene signature⁸ and potential intracellular targets of apigenin¹⁸. (B) *C1QTNF2* expression in a panel of various cell types isolated from mouse livers (expression DNA microarray, $n \geq 3$ in each cell type)⁸. BDL: bile duct ligation; CCl₄: carbon tetrachloride. * $p < 0.001$, Tukey's test. (C) Subcellular localization of *C1QTNF2* protein in TWNT-4 cells (immunofluorescence staining). (D) Modulation of *C1QTNF2* expression by apigenin and sorafenib in TWNT-4 cells (qRT-PCR, $n = 2$). (E) Modulation of *C1QTNF2* protein by apigenin and sorafenib in TWNT-4 cells and adipose tissues (Western blotting, $n = 1$). Relative intensity to tubulin was calculated.

chance is less than 1 (0.959), although it does not reach statistical significance ($p = 0.37$, hypergeometric test). To date, C1q and tumor necrosis factor related protein 2 encoded (*C1QTNF2*) protein is an adipokine that has been identified previously in adipose tissue, where it has effects on lipid metabolism and insulin activity¹⁹, but upregulation of *C1QTNF2* mRNA expression unique to HSC was confirmed in a panel of various cell types presenting in fibrotic liver, which were assembled in our previous study⁸ (Fig. 2B). Furthermore, immunofluorescence staining showed strong cytoplasmic expression of *C1QTNF2* in TWNT-4 cells (Fig. 2C). Apigenin treatment did not alter *C1QTNF2* mRNA and protein abundance (Fig. 2D,E). These results suggest that apigenin elicits its COL1A1-suppressive effect in HSC without modulating *C1QTNF2* expression levels. However, apigenin could interfere with the function of *C1QTNF2* protein via a physical interaction. Interestingly, baseline *C1QTNF2* mRNA expression was reduced during the process of *in vivo* HSC activation by carbon tetrachloride (CCl₄) treatment or bile duct ligation (BDL) (Fig. 2B) and *in vitro* culture activation¹³ (Fig. 3A). *C1QTNF2* protein expression was similarly reduced in the livers from mouse model of alcoholic injury by Lieber DeCarli ethanol-containing diet for 6 weeks²⁰ (Fig. 3B). Furthermore, in a clinical cohort of 216 patients with HCV-related compensated cirrhosis, patients with high *C1QTNF2* expression showed a better clinical outcome of cirrhosis, as measured by Child-Pugh classification²¹ (Fig. 4). These animal model- and clinical cohort-based findings suggest that *C1QTNF2* plays a protective role in cirrhosis progression. If a physical interaction with *C1QTNF2* protein

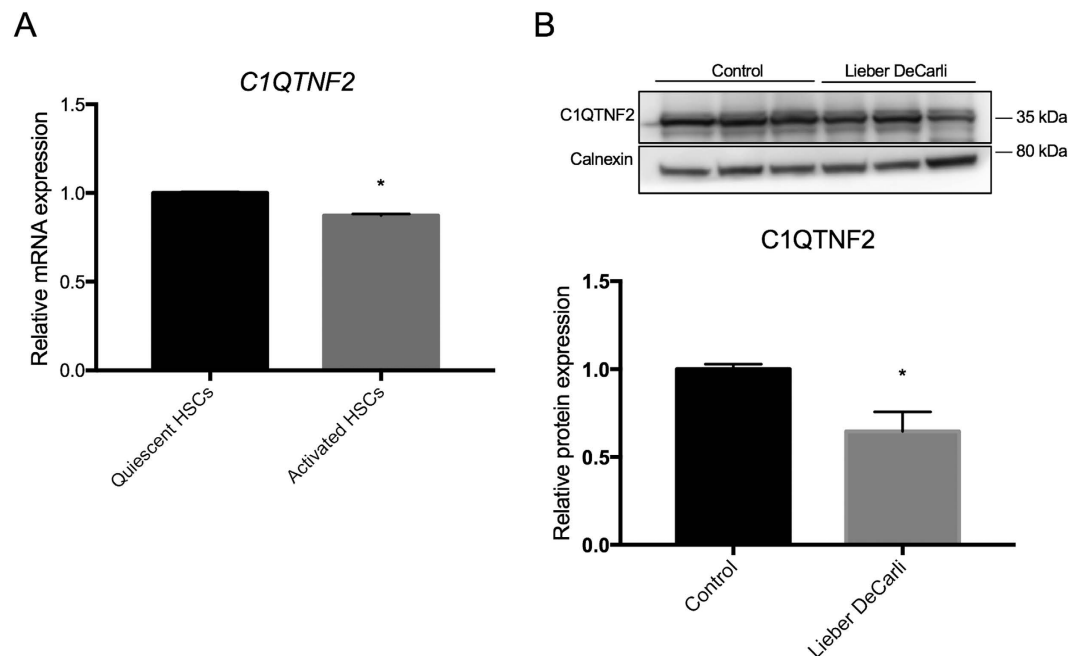


Figure 3. Reduced C1QTNF2 mRNA and protein expression in mouse primary HSCs and ethanol-injured liver. (A) *C1QTNF2* expression in freshly isolated (“quiescent”) and 7-day-cultured (“activated”) mouse primary HSCs¹³ (expression DNA microarray, $n = 3$). * $p < 0.001$, t-test. (B) *C1QTNF2* protein expression in livers from mice fed with Lieber DeCarli ethanol-containing diet normalized to calnexin (Western blotting, $n = 5$). * $p < 0.05$, t-test. Bar graphs show mean and standard error of mean (SEM) (error bars) of replicated experiments.

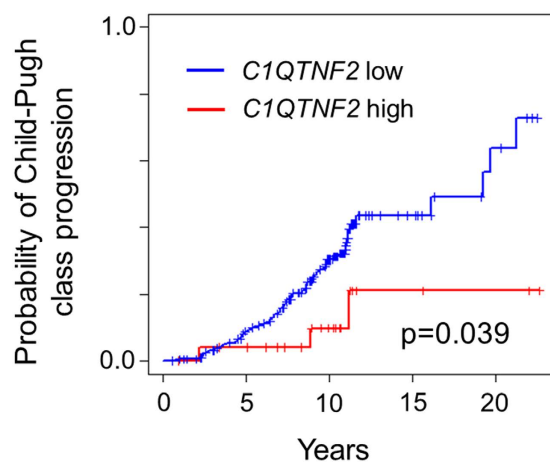


Figure 4. Prognostic association of *C1QTNF2* expression in a clinical HCV cirrhosis cohort. (A) clinical cohort of 216 patients with compensated HCV-related cirrhosis⁶ was classified into *C1QTNF2*-high ($n = 25$) and low ($n = 101$) groups, and evaluated for association with cirrhosis progression, i.e., progression of Child-Pugh class²¹ from (A) to (B) or (C). P-value was calculated by log-rank test.

is needed for apigenin to elicit its *COL1A1*-suppressive effect as we computationally predict, it may be possible that the status of *C1QTNF2* expression can serve as a predictive marker of apigenin responses, which could be clarified in future studies.

Discussion

Molecular signature-based unbiased and hypothesis-free computational drug discovery has been successfully utilized primarily in cancer and inflammatory diseases³. Our study has demonstrated that this strategy can be similarly applied to anti-fibrotic drug discovery. Generation of the query gene signature in transcriptomic profiles of activated HSCs enabled the discovery of candidate compounds specific to the biological context, circumventing the need for costly large compound library screen. The identification of apigenin, already known to be

anti-fibrotic in other tissue types such as pancreas^{22,23}, clearly indicates that our approach is a viable option to discover biologically relevant anti-fibrotic agents in a cost-effective manner.

Apigenin is a flavonoid, abundant in parsley and celery, that has gained interest as a health-promoting agent because of its low intrinsic toxicity²⁴. Despite the promising *in vitro* anti-fibrogenic activity comparable to sorafenib¹⁴, its poor solubility limits optimal *in vivo* biodistribution and needs further biochemical modifications to improve solubility. In addition, apigenin is known to modulate the immune response¹⁸, although our *in vitro* experimental system did not uncover an immune-related activity, which could be assessed in future studies. C1QTNF2, which we have associated with liver disease severity and prognosis, may be a factor that potentially influences the outcome of apigenin-based therapy in particular, and the biology of hepatic fibrosis in general. C1QTNF2 is a member of C1q/TNF-related proteins that represent an adipokine family less characterized than other well-studied adipocytokines implicated in liver fibrosis, such as adiponectin^{19,25}. The only known source of C1QTNF2 production is stromal vascular cells in adipose tissue, and the highly restricted sites of production suggests its function is distinct from adiponectin¹⁹. Indeed, C1QTNF2 does not substitute for adiponectin in caloric restriction²⁶. C1QTNF2 is known to be involved in several metabolic processes such as AMP kinase phosphorylation to stimulate glucose uptake in muscle cells²⁷ and improvement of insulin and lipid tolerance in diet-induced obese mice²⁸. C1QTNF2 may form heteromers with C1QTNF7 and adiponectin¹⁹. Our study suggests it has a novel role in HSC biology that could maintain the cell's quiescent state. These findings reinforce the value of computational approaches to drug discovery for hepatic fibrosis, and identify C1QTNF2 as a potential mediator of apigenin's anti-fibrotic activity.

References

1. Mederacke, I. *et al.* Fate tracing reveals hepatic stellate cells as dominant contributors to liver fibrosis independent of its aetiology. *Nat Commun* **4**, 2823 (2013).
2. Trautwein, C., Friedman, S. L., Schuppan, D. & Pinzani, M. Hepatic fibrosis: Concept to treatment. *J Hepatol* **62**, S15–24 (2015).
3. Wooden, B., Goossens, N., Hoshida, Y. & Friedman, S. L. Using Big Data to Discover Diagnostics and Therapeutics for Gastrointestinal and Liver Diseases. *Gastroenterology* **152**, 53–67 e53 (2017).
4. Blaauboer, M. E. *et al.* Novel combination of collagen dynamics analysis and transcriptional profiling reveals fibrosis-relevant genes and pathways. *Matrix Biol* **32**, 424–431 (2013).
5. Hoshida, Y. *et al.* Integrative transcriptome analysis reveals common molecular subclasses of human hepatocellular carcinoma. *Cancer Res* **69**, 7385–7392 (2009).
6. Hoshida, Y. *et al.* Prognostic gene expression signature for patients with hepatitis C-related early-stage cirrhosis. *Gastroenterology* **144**, 1024–1030 (2013).
7. Hoshida, Y. *et al.* Gene expression in fixed tissues and outcome in hepatocellular carcinoma. *N Engl J Med* **359**, 1995–2004 (2008).
8. Zhang, D. Y. *et al.* A hepatic stellate cell gene expression signature associated with outcomes in hepatitis C cirrhosis and hepatocellular carcinoma after curative resection. *Gut* **65**, 1754–1764 (2016).
9. Fuchs, B. C. *et al.* Epidermal growth factor receptor inhibition attenuates liver fibrosis and development of hepatocellular carcinoma. *Hepatology* **59**, 1577–1590 (2014).
10. Lamb, J. *et al.* The Connectivity Map: using gene-expression signatures to connect small molecules, genes, and disease. *Science* **313**, 1929–1935 (2006).
11. Shibata, N. *et al.* Establishment of an immortalized human hepatic stellate cell line to develop antifibrotic therapies. *Cell transplantation* **12**, 499–507 (2003).
12. Friedman, S. L. & Roll, F. J. Isolation and culture of hepatic lipocytes, Kupffer cells, and sinusoidal endothelial cells by density gradient centrifugation with Stractan. *Analytical biochemistry* **161**, 207–218 (1987).
13. Chen, Y. *et al.* Hedgehog controls hepatic stellate cell fate by regulating metabolism. *Gastroenterology* **143**, 1319–1329 e1311–1311 (2012).
14. Thabut, D. *et al.* Complementary vascular and matrix regulatory pathways underlie the beneficial mechanism of action of sorafenib in liver fibrosis. *Hepatology* **54**, 573–585 (2011).
15. Bridle, K. R. *et al.* Rapamycin inhibits hepatic fibrosis in rats by attenuating multiple profibrogenic pathways. *Liver Transplantation* **15**, 1315–1324 (2009).
16. Chen, H. *et al.* Design, synthesis, and characterization of novel apigenin analogues that suppress pancreatic stellate cell proliferation *in vitro* and associated pancreatic fibrosis *in vivo*. *Bioorganic & medicinal chemistry* **22**, 3393–3404 (2014).
17. Mrazek, A. A. *et al.* Apigenin inhibits pancreatic stellate cell activity in pancreatitis. *Journal of Surgical Research* **196**, 8–16 (2015).
18. Arango, D. *et al.* Molecular basis for the action of a dietary flavonoid revealed by the comprehensive identification of apigenin human targets. *Proc Natl Acad Sci USA* **110**, E2153–2162 (2013).
19. Wong, G. W. *et al.* Molecular, biochemical and functional characterizations of C1q/TNF family members: adipose-tissue-selective expression patterns, regulation by PPAR-gamma agonist, cysteine-mediated oligomerizations, combinatorial associations and metabolic functions. *Biochem J* **416**, 161–177 (2008).
20. Lieber, C. S. & DeCarli, L. M. The feeding of alcohol in liquid diets: two decades of applications and 1982 update. *Alcohol Clin Exp Res* **6**, 523–531 (1982).
21. Pugh, R. N., Murray-Lyon, I. M., Dawson, J. L., Pietroni, M. C. & Williams, R. Transection of the oesophagus for bleeding oesophageal varices. *Br J Surg* **60**, 646–649 (1973).
22. Chen, H. *et al.* Design, synthesis, and characterization of novel apigenin analogues that suppress pancreatic stellate cell proliferation *in vitro* and associated pancreatic fibrosis *in vivo*. *Bioorg Med Chem* **22**, 3393–3404 (2014).
23. Mrazek, A. A. *et al.* Apigenin inhibits pancreatic stellate cell activity in pancreatitis. *J Surg Res* **196**, 8–16 (2015).
24. Shukla, S. & Gupta, S. Apigenin: a promising molecule for cancer prevention. *Pharmaceutical research* **27**, 962–978 (2010).
25. Schaffler, A. & Buechler, C. CTRP family: linking immunity to metabolism. *Trends Endocrinol Metab* **23**, 194–204 (2012).
26. Rohrbach, S., Aurich, A. C., Li, L. & Niemann, B. Age-associated loss in adiponectin-activation by caloric restriction: lack of compensation by enhanced inducibility of adiponectin paralogs CTRP2 and CTRP7. *Mol Cell Endocrinol* **277**, 26–34 (2007).
27. Wong, G. W., Wang, J., Hug, C., Tsao, T.-S. & Lodish, H. F. A family of Acrp30/adiponectin structural and functional paralogs. *Proceedings of the National Academy of Sciences of the United States of America* **101**, 10302–10307 (2004).
28. Peterson, J. M., Seldin, M. M., Tan, S. Y. & Wong, G. W. CTRP2 overexpression improves insulin and lipid tolerance in diet-induced obese mice. *PLoS One* **9**, e88535 (2014).
29. Smolen, J. S. *et al.* Efficacy and safety of leflunomide compared with placebo and sulphasalazine in active rheumatoid arthritis: a double-blind, randomised, multicentre trial. *The Lancet* **353**, 259–266 (1999).
30. Lane, I., Lumley, P., Michael, M., Peters, A. & McCollum, C. A specific thromboxane receptor blocking drug, AH23848, reduces platelet deposition on vascular grafts in man. *Thrombosis and haemostasis* **64**, 369–373 (1990).

31. De Bono, D. P. *et al.* Effect of the specific thromboxane receptor blocking drug AH23848 in patients with angina pectoris. *British heart journal* **56**, 509–517 (1986).
32. German & Group, A.X.S. Double-blind placebo-controlled comparison of digoxin and xamoterol in chronic heart failure. *The Lancet* **331**, 489–493 (1988).
33. Rougier, P. *et al.* Phase II study of irinotecan in the treatment of advanced colorectal cancer in chemotherapy-naïve patients and patients pretreated with fluorouracil-based chemotherapy. *Journal of Clinical Oncology* **15**, 251–260 (1997).
34. Pareek, A., Chandanwale, A., Oak, J., Jain, U. & Kapoor, S. Efficacy and safety of aceclofenac in the treatment of osteoarthritis: a randomized double-blind comparative clinical trial versus diclofenac—an Indian experience. *Current medical research and opinion* **22**, 977–988 (2006).
35. Sandoval, M. A. & Hernandez-Vaquero, D. Preventing peridural fibrosis with nonsteroidal anti-inflammatory drugs. *European Spine Journal* **17**, 451–455 (2008).
36. Singh, G., Radhakrishnan, G. & Guleria, K. Comparison of sublingual misoprostol, intravenous oxytocin, and intravenous methylergometrine in active management of the third stage of labor. *International Journal of Gynecology & Obstetrics* **107**, 130–134 (2009).
37. Bateman, B. *et al.* Methylergonovine Maleate and the Risk of Myocardial Ischemia and Infarction. *Obstetric Anesthesia Digest* **34**, 214–215 (2014).
38. Chung, F.-H. *et al.* Gene-Set Local Hierarchical Clustering (GSLHC)—A Gene Set-Based Approach for Characterizing Bioactive Compounds in Terms of Biological Functional Groups. *PLoS one* **10**, e0139889 (2015).
39. Investigators, W.G.f.t.W.s.H.I. Risks and benefits of estrogen plus progestin in healthy postmenopausal women: principal results from the Women's Health Initiative randomized controlled trial. *Jama* **288**, 321–333 (2002).
40. Janssen, K. *et al.* Effects of the flavonoids quercetin and apigenin on hemostasis in healthy volunteers: results from an *in vitro* and a dietary supplement study. *The American journal of clinical nutrition* **67**, 255–262 (1998).
41. Ma, G., Zhang, R., Ying, K. & Wang, D. Effect evaluation of cisplatin-gemcitabine combination chemotherapy for advanced non-small cell lung cancer patients using microarray data. *Eur Rev Med Pharmacol Sci* **19**, 578–585 (2015).
42. Li, J. *et al.* Gene expression profiling of CD133-positive cells in coronary artery disease. *Molecular medicine reports* **12**, 7512–7516 (2015).
43. Balakumar, P. & Singh, M. Effect of 3-aminobenzamide, an inhibitor of poly (ADP-ribose) polymerase in experimental cardiac hypertrophy. *Int J Pharmacol* **2**, 543–548 (2006).
44. Huttunen, M. O. *et al.* Risperidone versus zuclopenthixol in the treatment of acute schizophrenic episodes: a double-blind parallel-group trial. *Acta Psychiatrica Scandinavica* **91**, 271–277 (1995).
45. Yoshitake, T., Asano, K., Yamamura, H., Yoshitake, J. & Arai, T. Experimental and clinical studies on the hemodynamic and metabolic effects of dibutyl cyclic AMP. *Progress in clinical and biological research* **111**, 211 (1983).
46. Miyagi, Y., Sasayama, S., Nakajima, H., Fujita, M. & Asanoi, H. Comparative hemodynamic effects of intravenous dobutamine and dibutyl cyclic AMP, a new inotropic agent, in severe congestive heart failure. *Journal of cardiovascular pharmacology* **15**, 138–143 (1990).
47. Kollros, P., Bates, S., Mathews, M., Horwitz, A. & Glagov, S. Cyclic AMP inhibits increased collagen production by cyclically stretched smooth muscle cells. *Laboratory investigation; a journal of technical methods and pathology* **56**, 410–417 (1987).

Acknowledgements

Funding from Icahn School of Medicine Medical Student Research Office to D.F.H. Juan de la Cierva contract (JCI-2012-15124, Ministerio de Economía y Competitividad) and Fundación Juan Esplugues and FISABIO (UGP-14-153) to A.B.G. FLAGS foundation, the Nuovo-Soldati Cancer Research Foundation, and an advanced training grant from Geneva University Hospital to N.G. NIH/NIDDK DK099558, European Union ERC-2014-AdG-671231HEPCIR, Irma T. Hirsch Trust, and US Department of Defense (W81XWH-16-1-0363) to Y.H., and NIH DK56621 and AA020709 to S.L.F.

Author Contributions

Study concept and design: D.F.H., N.G., A.B.G., B.W., M.C.W., B.R., J.T.D., Y.A.L., Y.H., S.L.F. Acquisition of data: D.F.H., N.G., A.B.G., T.T., M.C.W., A.L., B.R. Analysis and interpretation of data: D.F.H., N.G., A.B.G., M.C.W., A.L., Y.A.L., Y.H., S.L.F. Drafting of the manuscript: D.F.H., Y.H., S.L.F. Critical revision of the manuscript for important intellectual content: all authors. Obtained funding: D.F.H., N.G., T.T., Y.H., S.L.F.

Additional Information

Supplementary information accompanies this paper at <http://www.nature.com/srep>

Competing financial interests: The authors declare no competing financial interests.

How to cite this article: Hicks, D. F. *et al.* Transcriptome-based repurposing of apigenin as a potential anti-fibrotic agent targeting hepatic stellate cells. *Sci. Rep.* **7**, 42563; doi: 10.1038/srep42563 (2017).

Publisher's note: Springer Nature remains neutral with regard to jurisdictional claims in published maps and institutional affiliations.



This work is licensed under a Creative Commons Attribution 4.0 International License. The images or other third party material in this article are included in the article's Creative Commons license, unless indicated otherwise in the credit line; if the material is not included under the Creative Commons license, users will need to obtain permission from the license holder to reproduce the material. To view a copy of this license, visit <http://creativecommons.org/licenses/by/4.0/>

© The Author(s) 2017